Results in Physics 23 (2021) 104019

Contents lists available at ScienceDirect

Results in Physics

journal homepage: www.elsevier.com/locate/rinp

Accurate novel explicit complex wave solutions of the (2+1)-dimensional Chiral nonlinear Schrödinger equation

B. Alshahrani [a], H.A. Yakout [a], Mostafa M.A. Khater [b,c], Abdel-Haleem Abdel-Aty [d,e,*], Emad E. Mahmoud [f], Dumitru Baleanu [g,h], Hichem Eleuch [i,j,k]

[a] Department of Physics, College of Sciences, King Khalid University, Abha 61413, Saudi Arabia
[b] Department of Mathematics, Faculty of Science, Jiangsu University, 212013 Zhenjiang, China
[c] Department of Mathematics, Obour High Institute For Engineering and Technology, 11828 Cairo, Egypt
[d] Department of Physics, College of Sciences, University of Bisha, P.O. Box 344, Bisha 61922, Saudi Arabia
[e] Physics Department, Faculty of Science, Al-Azhar University, Assiut 71524, Egypt
[f] Department of Mathematics and Statistics, College of Science, Taif University, PO Box 11099, Taif 21944, Saudi Arabia
[g] Institute of Space Sciences, Magurele-Bucharest, Romania
[h] Department of Medical Research, China Medical University Hospital, China Medical University, Taichung, Taiwan
[i] Department of Applied Physics and Astronomy, University of Sharjah, Sharjah, United Arab Emirates
[j] College of Arts and Sciences, Abu Dhabi University, Abu Dhabi 59911, United Arab Emirates
[k] Institute for Quantum Science and Engineering, Texas A&M University, College Station, TX 77843, USA

ARTICLE INFO

Keywords:
(2+1)-dimensional nonlinear Chiral Schrödinger equation
Computational and approximate simulations
Complex solitary wave solutions

Mathematics subject classification:
35E05
35Q51
35Q92

ABSTRACT

This manuscript investigates the accuracy of the solitary wave solutions of the (2+1)-dimensional nonlinear Chiral Schrödinger ((2+1)-D CNLS) equation that are constructed by employing two recent analytical techniques (modified Khater (MKhat) and modified Jacobian expansion (MJE) methods). This investigation is based on evaluating the initial and boundary conditions through the obtained analytical solutions then employing the Adomian decomposition (AD) method to evaluate the approximate solutions of the (2+1)-D CNLS equation. This framework gives the ability to get large complex traveling wave solutions of the considered model and shows the superiority of the employed computational schemes by comparing the absolute error for each of them. The handled model describes the edge states of the fractional quantum hall effect. Many novel solutions are obtained with various formulas such as trigonometric, rational, and hyperbolic to the studied model. For more illustration of the results, some solutions are displayed in 2D, 3D, and density plots.

1. Introduction

Many fields have recently given great attention to soliton theory where it is relevant in fiber optics, biology, magnets, nuclear physics, etc [1–8]. This kind of wave often appears in shallow water, either in a lakeshore or rivers, since isolating the waves in the shallow water is considered a primary reason for creating the soliton waves [9]. Soliton waves are branched to many types, but the optical soliton waves are fundamental waves over all other types of soliton waves because of their typical plasma physics applications [10–15]. Many mathematical equations have been formulated for admitting soliton solutions, such as KdV and Kadomtsev–Petviashvili (KP) equations, to study the local ion density in the perturbation of charge density [16–18]. Consequently, many researchers have given a significant focus on studying soliton behavior in plasma physics [19–21]. Many novel characterizations of the optical soliton wave have been discovered, such as its ability to propagate without distortion over long distances [22,23]. This optical soliton wave behavior is beneficial, especially in the communication area, pulse compression, logic gates, photonic switches, pulse amplification, timing jitter, and fiber laser, to provide high-rate communication through an optical fiber [24,25]. So far, soliton waves are considered as an incompletely discovered field as it's unknown dynamical behavior in metamaterials [26,27].

In this context, the well–known cubic nonlinear Schrödinger equation has attracted several researchers in this field because of its ability to investigate the spread of pulses in Kerr media and specifically in quantum physics [28,29]. This equation can also illustrate the edge states of the fractional quantum hall effect [30]. Anomalous dispersion and self-

* Corresponding author at: Department of Physics, College of Sciences, University of Bisha, P.O. Box 344, Bisha 61922, Saudi Arabia.
E-mail addresses: bserhany@kku.edu.sa (B. Alshahrani), amabdelaty@ub.edu.sa (A.-H. Abdel-Aty), e.mahmoud@tu.edu.sa (E.E. Mahmoud).

https://doi.org/10.1016/j.rinp.2021.104019
Received 12 January 2021; Received in revised form 17 February 2021; Accepted 25 February 2021
Available online 12 March 2021
2211-3797/© 2021 The Author(s). Published by Elsevier B.V. This is an open access article under the CC BY-NC-ND license (http://creativecommons.org/licenses/by-nc-nd/4.0/).

phase modulation give the Kerr effect on attaining a chirp frequency [31]. Balancing between the nonlinear influence contributes and dispersion leads to a free–chirp pulse output [32]. Studying the distribution of pulses in pico–second systems is explained clearly and in–details through nonlinear Schrödinger equation [33]. Increasing in incident power gives the higher-order dispersion, and non-Kerr nonlinearity, extraordinary significance in ultra–short pulses [34].

In this paper, the solitary wave solutions of the (2+1)-D CNLS equation which is given by [35]

$$i\mathscr{S}_t + r_1\left(\mathscr{S}_{xx} + \mathscr{S}_{yy}\right) + i\left(r_2\left(\mathscr{S}\mathscr{Q}_x - \mathscr{Q}\mathscr{S}_x\right) + r_3\left(\mathscr{S}\mathscr{Q}_y - \mathscr{Q}\mathscr{S}_y\right)\mathscr{S}\right) = 0, \tag{1}$$

where $r_1, r_2 r_3$ are arbitrary constants to be calculated later which are representing respectively dispersion term, and nonlinear coupling constants while $\mathscr{S} = \mathscr{S}(x,y,t)$, $\mathscr{Q} = \mathscr{Q}(x,y,t)$. Handling Eq. (1) by implementing the next wave transformation $[\mathscr{S} = \psi(\mathfrak{Z})e^{tg_3+xg_1+yg_2+\mathscr{L}_1}$, $\mathscr{Q} = \psi(\mathfrak{Z})e^- itg_3 + xg_1 + yg_2 + \mathscr{L}_1, tg_6 + xg_4 + yg_5 + \mathscr{L}_2$, where $g_1, g_2, g_3, g_4, g_5, g_6, \mathscr{L}_1$, $\mathscr{L}_2$ are arbitrary constants to be evaluated later$]$, converts Eq. (1) into a real and imaginary parts, respectively

$$\begin{cases} \text{Re}: & k_2\psi'' + k_1\psi + \psi^3 = 0, \\ \text{Im}: & (2r_1(g_1g_4 + g_2g_5) + g_6)\psi' = 0, \end{cases} \tag{2}$$

where $\left[k_1 = \frac{-r_1g_1^2 - r_1g_2^2 - g_3}{2r_2g_1 + 2r_3g_2},\ k_2 = \frac{r_1g_4^2 + r_1g_5^2}{2r_2g_1 + 2r_3g_2}\right.$ where $2r_2g_1 + 2r_3g_2 \neq 0, -r_1g_1^2 - r_1g_2^2 - g_3 \neq 0, r_1g_4^2 + r_1g_5^2 \neq 0, g_6 = -2r_1(g_1g_4 + g_2g_5)\Big]$. Evaluating the balance between the terms of real part in Eq. (2) along the following suggested auxiliary equation of the employed computational (MKhat and MJE) schemes $\Big[f'(\mathfrak{Z}) = \frac{1}{\ln(\mathscr{M})}$

$$\left(d_2 + d_1\mathscr{M}^{-f(\mathfrak{Z})} + d_3\mathscr{M}^{f(\mathfrak{Z})}\right) \& \phi'(\mathfrak{Z}) = \sqrt{p\phi(\mathfrak{Z})^2 + q\phi(\mathfrak{Z})^4 + \rho}\ \Big]$$

, get $n = 1$. Consequently, the solitary wave solutions of the (2+1)-D CNLS equation are given by

$$\psi(\mathfrak{Z}) = \begin{cases} \sum_{i=1}^{n} a_i\mathscr{M}^{if(\mathfrak{Z})} + \sum_{i=1}^{n} b_i\mathscr{M}^{-if(\mathfrak{Z})} + a_0 = a_1\mathscr{M}^{f(\mathfrak{Z})} + a_0 + b_1\mathscr{M}^{-f(\mathfrak{Z})}, \\ \sum_{i=1}^{n} a_i\phi(\mathfrak{Z})^i + \sum_{i=1}^{n} b_i\phi(\mathfrak{Z})^{-i} + a_0 = a_1\phi(\mathfrak{Z}) + a_0 + \frac{b_1}{\phi(\mathfrak{Z})}. \end{cases} \tag{3}$$

Using the general solutions (3) on the real part in Eq. (2) to determine the value of the above–mentioned parameters, gets the parameters' values.

The rest paper's structure is given as follows; Section 2 obtains the solitary wave solutions of the (2+1)-D CNLS equation. Additionally, the accuracy of the analytical results is investigated. The solutions are displayed in 2D, 3D, and density plots. Furthermore, the matching between analytical and numerical solutions is explained through some 2D plots. Section 4 explains the results and originality of this paper. Section 5 presents the conclusion.

2. Explicit wave solutions

This section investigates solitary wave solutions through two recent computational (MKhat and MJE) techniques. Handling the converted nonlinear ordinary differential equation with the suggested methods' framework we get:

2.1. Mkhat technique's solutions

The above–mentioned parameters have been evaluated as follows:

Set I

$$a_1 \to \frac{2a_0d_3}{d_2}, b_1 \to 0, k_1 \to -\frac{a_0^2\left(d_2^2 - 4d_1d_3\right)}{d_2^2}, k_2 \to -\frac{2a_0^2}{d_2^2}.$$

Set II

$$a_1 \to 0, b_1 \to \frac{2a_0d_1}{d_2}, k_1 \to -\frac{a_0^2\left(d_2^2 - 4d_1d_3\right)}{d_2^2}, k_2 \to -\frac{2a_0^2}{d_2^2}.$$

Thus, the solitary wave solutions of the studied model are given by:

For $d_2^2 - 4d_1d_3 < 0, d_3 \neq 0$, we get

$$\mathscr{S}_{I,1}(x,y,t) = \frac{a_0\sqrt{4d_1d_3 - d_2^2}}{d_2}\tan\left(\frac{1}{2}\sqrt{4d_1d_3 - d_2^2}\,(tg_6 + xg_4 + yg_5 + \mathscr{L}_2)\right)e^{i(tg_3+xg_1+yg_2+\mathscr{L}_1)}, \tag{4}$$

$$\mathscr{S}_{I,2}(x,y,t) = \frac{a_0\sqrt{4d_1d_3 - d_2^2}}{d_2}\cot\left(\frac{1}{2}\sqrt{4d_1d_3 - d_2^2}\,(tg_6 + xg_4 + yg_5 + \mathscr{L}_2)\right)e^{i(tg_3+xg_1+yg_2+\mathscr{L}_1)}, \tag{5}$$

$$\mathscr{S}_{II,1}(x,y,t) = a_0e^{i(tg_3+xg_1+yg_2+\mathscr{L}_1)}\left(1 - \frac{4d_1d_3}{d_2^2 - d_2\sqrt{4d_1d_3 - d_2^2}\tan\left(\frac{1}{2}\sqrt{4d_1d_3 - d_2^2}\,(tg_6 + xg_4 + yg_5 + \mathscr{L}_2)\right)}\right), \tag{6}$$

$$\mathscr{S}_{\mathrm{II},2}(x,y,t)=a_0e^{i(tg_3+xg_1+yg_2+\mathscr{L}_1)}\left(1-\frac{4d_1d_3}{d_2^2-d_2\sqrt{4d_1d_3-d_2^2}\cot\left(\frac{1}{2}\sqrt{4d_1d_3-d_2^2}\,(tg_6+xg_4+yg_5+\mathscr{L}_2)\right)}\right). \tag{7}$$

For $d_2^2-4d_1d_3>0,\ d_3\neq 0$, we get

$$\mathscr{S}_{\mathrm{I},3}(x,y,t)=-\frac{a_0\sqrt{d_2^2-4d_1d_3}e^{i(tg_3+xg_1+yg_2+\mathscr{L}_1)}\tanh\left(\frac{1}{2}\sqrt{d_2^2-4d_1d_3}\,(tg_6+xg_4+yg_5+\mathscr{L}_2)\right)}{d_2}, \tag{8}$$

$$\mathscr{S}_{\mathrm{I},4}(x,y,t)=-\frac{a_0\sqrt{d_2^2-4d_1d_3}e^{i(tg_3+xg_1+yg_2+\mathscr{L}_1)}\coth\left(\frac{1}{2}\sqrt{d_2^2-4d_1d_3}\,(tg_6+xg_4+yg_5+\mathscr{L}_2)\right)}{d_2}, \tag{9}$$

$$\mathscr{S}_{\mathrm{II},3}(x,y,t)=a_0e^{i(tg_3+xg_1+yg_2+\mathscr{L}_1)}\left(1-\frac{4d_1d_3}{d_2^2+\sqrt{d_2^2-4d_1d_3}\,d_2\tanh\left(\frac{1}{2}\sqrt{d_2^2-4d_1d_3}\,(tg_6+xg_4+yg_5+\mathscr{L}_2)\right)}\right), \tag{10}$$

$$\mathscr{S}_{\mathrm{II},4}(x,y,t)=a_0e^{i(tg_3+xg_1+yg_2+\mathscr{L}_1)}\left(1-\frac{4d_1d_3}{d_2^2+\sqrt{d_2^2-4d_1d_3}\,d_2\coth\left(\frac{1}{2}\sqrt{d_2^2-4d_1d_3}\,(tg_6+xg_4+yg_5+\mathscr{L}_2)\right)}\right). \tag{11}$$

For $d_2=d_3=\kappa,\ d_1=0$, we get

$$\mathscr{S}_{\mathrm{I},5}(x,y,t)=a_0\left(-e^{i(tg_3+xg_1+yg_2+\mathscr{L}_1)}\right)\coth\left(\frac{1}{2}\kappa(tg_6+xg_4+yg_5+\mathscr{L}_2)\right). \tag{12}$$

For $d_2=\frac{d_1}{2}=\kappa,\ d_3=0$, we get

$$\mathscr{S}_{\mathrm{II},5}(x,y,t)=a_0e^{i(tg_3+xg_1+yg_2+\mathscr{L}_1)}\left(\frac{4}{e^{\kappa(tg_6+xg_4+yg_5+\mathscr{L}_2)}-2}+1\right). \tag{13}$$

For $d_1=0,\ d_2\neq 0,\ d_3\neq 0$, we get

$$\mathscr{S}_{\mathrm{I},6}(x,y,t)=-\frac{a_0e^{i(tg_3+xg_1+yg_2+\mathscr{L}_1)}\left(d_3e^{d_2(tg_6+xg_4+yg_5+\mathscr{L}_2)}+2\right)}{d_3e^{d_2(tg_6+xg_4+yg_5+\mathscr{L}_2)}-2}. \tag{14}$$

For $d_3=0,\ d_2\neq 0,\ d_1\neq 0$, we get

$$\mathscr{S}_{\mathrm{II},6}(x,y,t)=a_0e^{i(tg_3+xg_1+yg_2+\mathscr{L}_1)}\left(1-\frac{2d_1}{d_1-d_2e^{d_2(tg_6+xg_4+yg_5+\mathscr{L}_2)}}\right). \tag{15}$$

2.2. MJE technique's solutions

For this technique we obtain:

Set I

$$a_0\to 0,\ b_1\to-\frac{a_1\sqrt{\rho}}{\sqrt{q}},\ k_1\to\frac{a_1^2p+6a_1^2\sqrt{q}\sqrt{\rho}}{2q},\ k_2\to-\frac{a_1^2}{2q}.$$

Set II

$$a_0\to 0,\ b_1\to\frac{a_1\sqrt{\rho}}{\sqrt{q}},\ k_1\to\frac{a_1^2p-6a_1^2\sqrt{q}\sqrt{\rho}}{2q},\ k_2\to-\frac{a_1^2}{2q}.$$

Thus, the solitary wave solutions of the studied model are given by:

When $m=1$;

For $\rho\to 1, p\to -2, q\to 1$, we get

$$\mathscr{S}_{\mathrm{I},1}(x,y,t)=-2a_1e^{i(tg_3+xg_1+yg_2+\mathscr{L}_1)}\operatorname{csch}(2(tg_6+xg_4+yg_5+\mathscr{L}_2)), \tag{16}$$

$$\mathscr{S}_{\mathrm{II},1}(x,y,t)=a_1e^{i(tg_3+xg_1+yg_2+\mathscr{L}_1)}(\tanh(tg_6+xg_4+yg_5+\mathscr{L}_2)+\coth(tg_6+xg_4+yg_5+\mathscr{L}_2)). \tag{17}$$

For $\rho\to 0, p\to 1, q\to -1$, we get

$$\mathscr{S}_{\mathrm{I,II},2}(x,y,t)=a_1e^{i(tg_3+xg_1+yg_2+\mathscr{L}_1)}\operatorname{sech}(tg_6+xg_4+yg_5+\mathscr{L}_2). \tag{18}$$

For $\rho\to\frac{1}{4}, p\to-\frac{1}{2}, q\to\frac{1}{4}$, we get

$$\mathscr{S}_{\mathrm{I},3}(x,y,t)=\frac{a_1e^{i(tg_3+xg_1+yg_2+\mathscr{L}_1)}\left((\coth(tg_6+xg_4+yg_5+\mathscr{L}_2)\pm\operatorname{csch}(tg_6+xg_4+yg_5+\mathscr{L}_2))^2-1\right)}{\coth(tg_6+xg_4+yg_5+\mathscr{L}_2)\pm\operatorname{csch}(tg_6+xg_4+yg_5+\mathscr{L}_2)}, \tag{19}$$

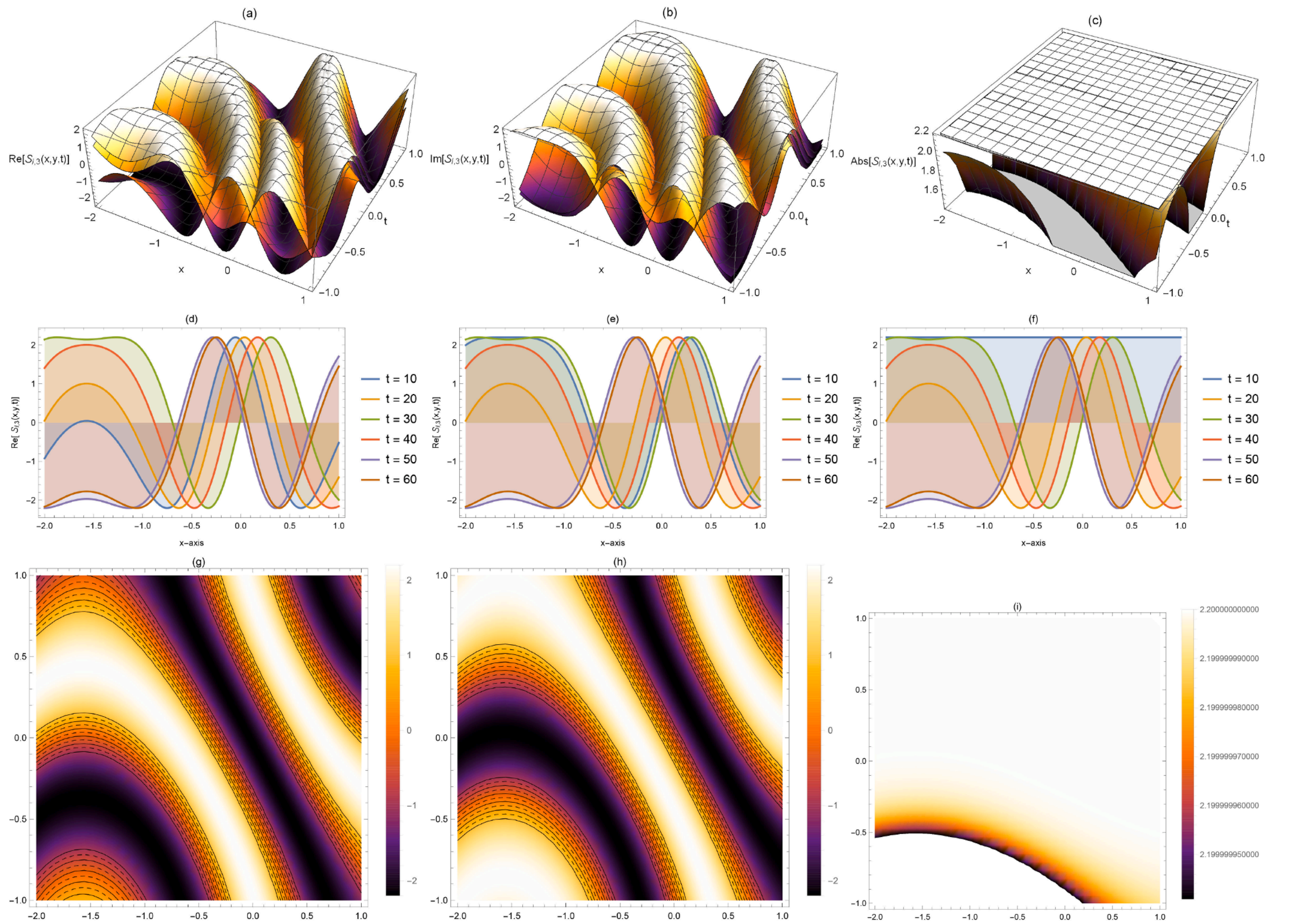

Fig. 1. Distinct plots in three, two–dimensional and contour plots of Eq. (8) for (a, d, g) real, (b, e, h) imaginary, and (c, f, i) absolute value of the solution with the following values $(a_0 = 11, d_2 = 5, d_1 = 3, d_3 = 2, g_1 = 5, g_2 = 6, g_3 = 4, g_4 = 3, g_5 = 9, g_6 = 10, \mathscr{L}_1 = 7, \mathscr{L}_2 = 8)$.

$$\mathscr{S}_{\mathrm{II},3}(x,y,t) = \frac{a_1 e^{i(tg_3+xg_1+yg_2+\mathscr{L}_1)}\left(\left(\coth(tg_6+xg_4+yg_5+\mathscr{L}_2) \pm \operatorname{csch}(tg_6+xg_4+yg_5+\mathscr{L}_2)\right)^2+1\right)}{\coth(tg_6+xg_4+yg_5+\mathscr{L}_2) \pm \operatorname{csch}(tg_6+xg_4+yg_5+\mathscr{L}_2)}. \tag{20}$$

For $\rho\to0, p\to1, q\to1$, we get

$$\mathscr{S}_{\mathrm{I,II},4}(x,y,t) = a_1 e^{i(tg_3+xg_1+yg_2+\mathscr{L}_1)}\operatorname{csch}(tg_6+xg_4+yg_5+\mathscr{L}_2). \tag{21}$$

When $m = 0$;

For $\rho\to\frac{1}{4}, p\to\frac{1}{2}, q\to\frac{1}{4}$, we get

$$\mathscr{S}_{\mathrm{I,II},6}(x,y,t) = \frac{a_1 e^{i(tg_3+xg_1+yg_2+\mathscr{L}_1)}\left(\left(\csc(tg_6+xg_4+yg_5+\mathscr{L}_2) \pm \cot(tg_6+xg_4+yg_5+\mathscr{L}_2)\right)^2-1\right)}{\csc(tg_6+xg_4+yg_5+\mathscr{L}_2) \pm \cot(tg_6+xg_4+yg_5+\mathscr{L}_2)}, \tag{22}$$

$$\mathscr{S}_{\mathrm{I,II},7}(x,y,t) = \frac{a_1 e^{i(tg_3+xg_1+yg_2+\mathscr{L}_1)}\left(\left(\sec(tg_6+xg_4+yg_5+\mathscr{L}_2) \pm \tan(tg_6+xg_4+yg_5+\mathscr{L}_2)\right)^2-1\right)}{\sec(tg_6+xg_4+yg_5+\mathscr{L}_2) \pm \tan(tg_6+xg_4+yg_5+\mathscr{L}_2)}. \tag{23}$$

For $\rho\to1, p\to2, q\to1$, we get

$$\mathscr{S}_{\mathrm{I},8}(x,y,t) = a_1 e^{i(tg_3+xg_1+yg_2+\mathscr{L}_1)}\left(\tan(tg_6+xg_4+yg_5+\mathscr{L}_2) - \cot(tg_6+xg_4+yg_5+\mathscr{L}_2)\right), \tag{24}$$

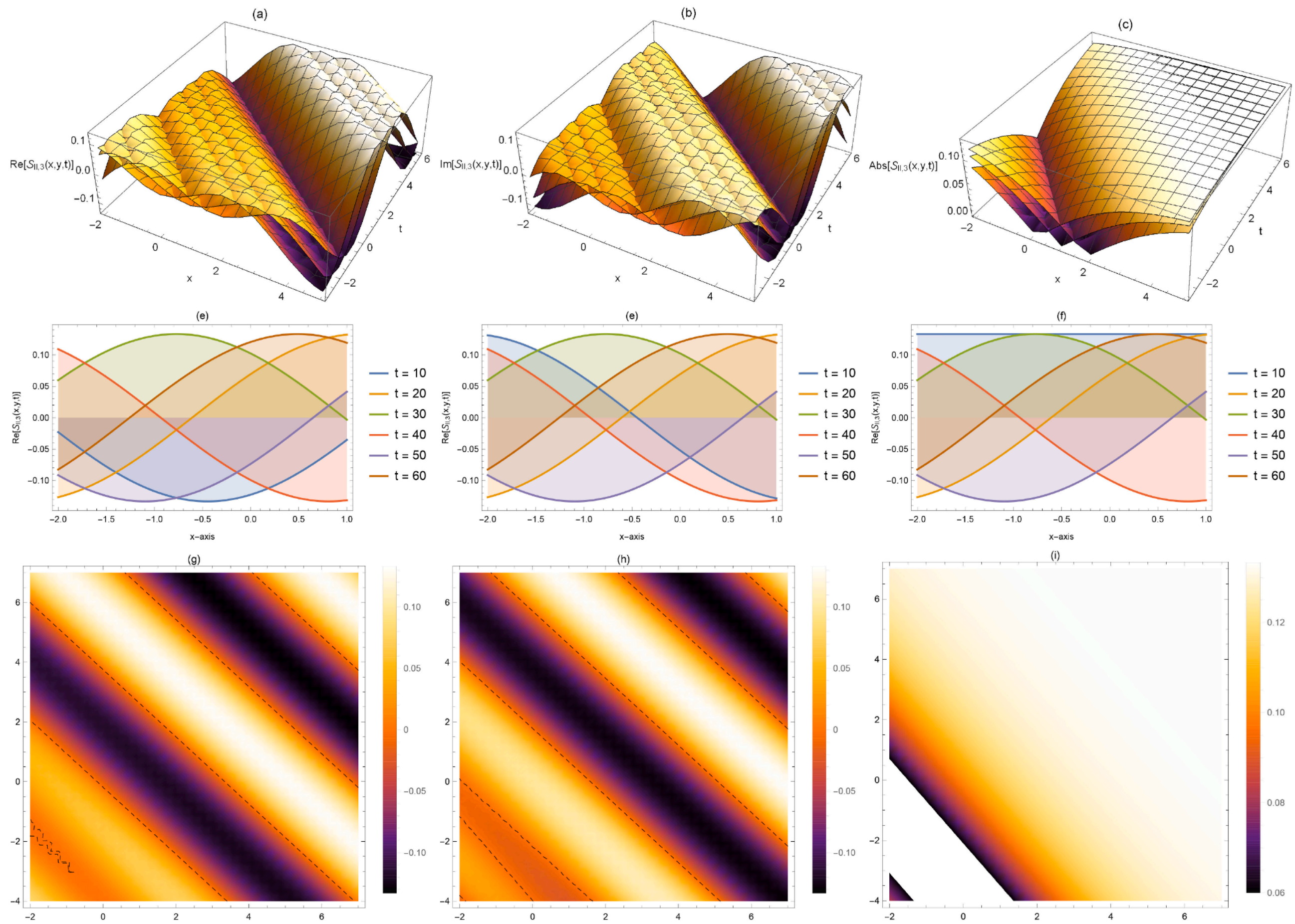

Fig. 2. Distinct plots in three, two–dimensional and contour plots of Eq. (10) for (a, d, g) real, (b, e, h) imaginary, and (c, f, i) absolute value of the solution with the following values $(a_0 = 0.4, d_2 = 3, d_1 = 2, d_3 = 1, g_1 = 0.9, g_2 = 0.8, g_3 = 0.8, g_4 = 0.7, g_5 = 0.6, g_6 = 0.5, \mathscr{L}_1 = 0.11, \mathscr{L}_2 = 0.1)$.

$$\mathscr{S}_{I,9}(x,y,t) = a_1 e^{i(tg_3+xg_1+yg_2+\mathscr{L}_1)}\tan(tg_6+xg_4+yg_5+\mathscr{L}_2)\big(\cot^2(tg_6+xg_4+yg_5+\mathscr{L}_2)-1\big), \tag{25}$$

$$\mathscr{S}_{II,8}(x,y,t) = 2a_1 e^{i(tg_3+xg_1+yg_2+\mathscr{L}_1)}\csc(2(tg_6+xg_4+yg_5+\mathscr{L}_2)), \tag{26}$$

3. Solutions' accuracy

Here, we investigate the accuracy of the constructed traveling wave solutions by implementing the AD semi–analytical schemes. This investigation depends on the evaluated solutions by the above–applied computational method to find the initial and boundary conditions. This study takes the following steps:

3.1. Accuracy of the Mkhat method's solution

Investigating Eq. (8) with the following value of the above–shown parameters $[a_0 = 7, d_2 = 5, d_1 = 3, d_3 = 2]$, we get the following solutions;

$$\mathscr{S}_0(\mathfrak{Z}) = -\frac{7\mathfrak{Z}}{10}, \tag{27}$$

$$\mathscr{S}_1(\mathfrak{Z}) = \frac{7\mathfrak{Z}^3}{120} - \frac{7\mathfrak{Z}^5}{1600}, \tag{28}$$

$$\mathscr{S}_2(\mathfrak{Z}) = \frac{49\mathfrak{Z}^{10}}{3840000} - \frac{7\mathfrak{Z}^8}{25600} + \frac{\mathfrak{Z}^7}{19200} - \frac{7\mathfrak{Z}^5}{4800}, \tag{29}$$

$$\mathscr{S}_3(\mathfrak{Z}) = -\frac{7\mathfrak{Z}^{13}}{106496000} - \frac{49\mathfrak{Z}^{12}}{1013760000} + \frac{7\mathfrak{Z}^{11}}{2816000} + \frac{7\mathfrak{Z}^{10}}{4608000} - \frac{67\mathfrak{Z}^9}{1382400} + \frac{31\mathfrak{Z}^7}{57600}, \tag{30}$$

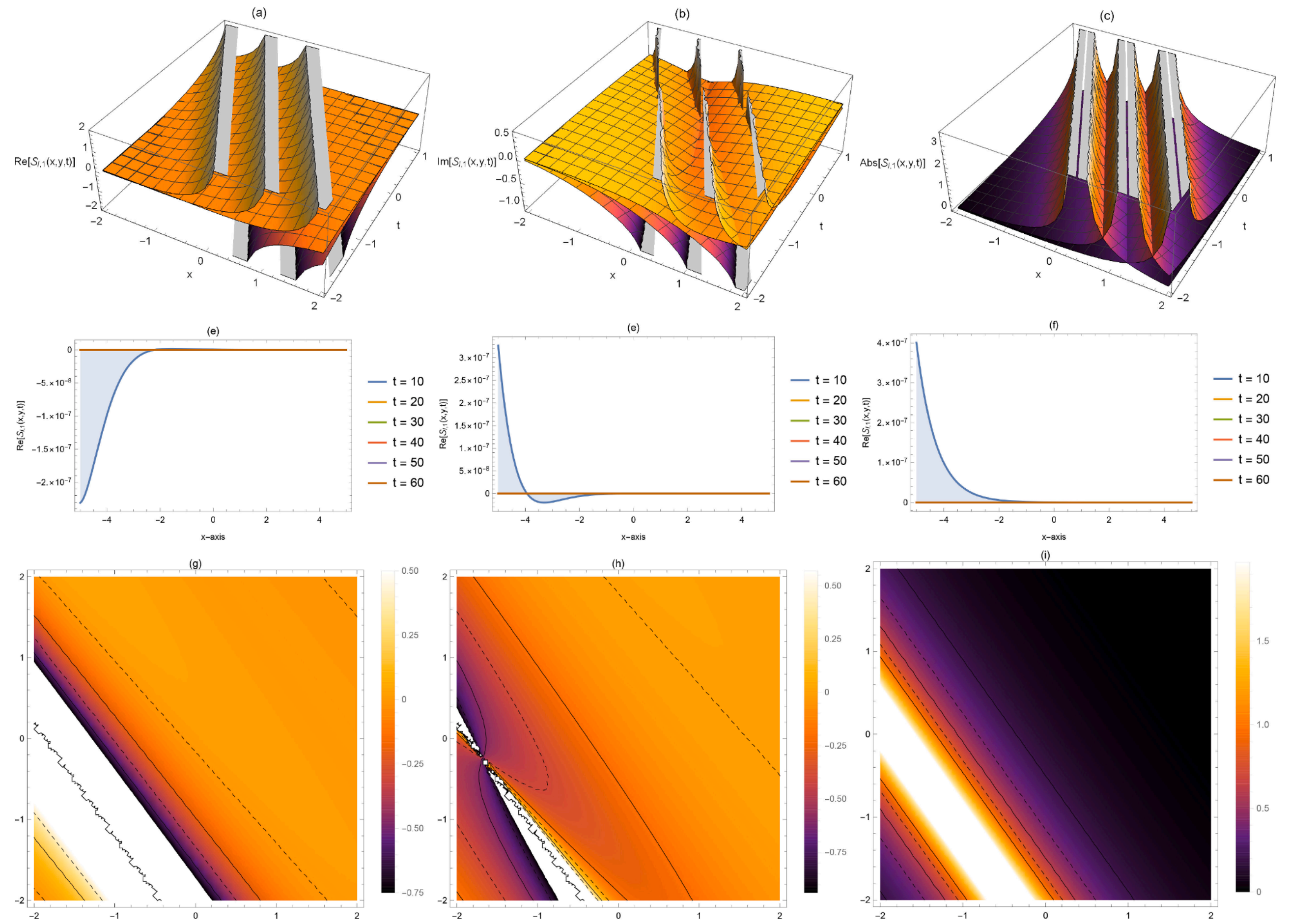

Fig. 3. Plots in three, two–dimensional and contour plots of Eq. (16) for (a, d, g) real, (b, e, h) imaginary, and (c, f, i) absolute value of the solution with the following values $(a_1 = 0.4, g_1 = 0.9, g_2 = 0.8, g_3 = 0.8, g_4 = 0.7, g_5 = 0.6, g_6 = 0.5, \mathscr{L}_1 = 0.11, \mathscr{L}_2 = 0.1)$.

Thus, the approximate solutions of the studied model based on the constructed solution via MKhat method is given by:

$$\mathscr{S}_{\text{App.}}(\mathfrak{z}) = -\frac{7\,\mathfrak{z}^{13}}{106496000} - \frac{49\,\mathfrak{z}^{12}}{1013760000} + \frac{7\,\mathfrak{z}^{11}}{2816000} + \frac{329\,\mathfrak{z}^{10}}{23040000} - \frac{67\,\mathfrak{z}^{9}}{1382400} - \frac{7\,\mathfrak{z}^{8}}{25600} + \frac{17\,\mathfrak{z}^{7}}{28800} - \frac{7\,\mathfrak{z}^{5}}{1200} + \frac{7\,\mathfrak{z}^{3}}{120} - \frac{7\,\mathfrak{z}}{10} + \cdots. \tag{31}$$

3.2. Accuracy of the MJE method's solution

Investigating Eq. (8) with the following value of the above–shown parameters $[a_1 = 7, p = 1, \rho = 0, q = -1]$, we get the following solutions;

$$\mathscr{S}_0(\mathfrak{z}) = 7, \tag{32}$$

$$\mathscr{S}_1(\mathfrak{z}) = -\frac{1}{2}(7\,\mathfrak{z}^2), \tag{33}$$

$$\mathscr{S}_2(\mathfrak{z}) = \frac{287\,\mathfrak{z}^4}{24}, \tag{34}$$

$$\mathscr{S}_3(\mathfrak{z}) = \frac{7\,\mathfrak{z}^6}{144} + \frac{7\,\mathfrak{z}^4}{4}, \tag{35}$$

Thus, the approximate solutions of the studied model based on the constructed solution via MJE method is given by:

$$\mathscr{S}_{\text{App.}}(\mathfrak{z}) = \frac{7\,\mathfrak{z}^6}{144} + \frac{329\,\mathfrak{z}^4}{24} - \frac{7\,\mathfrak{z}^2}{2} + 7 + \cdots. \tag{36}$$

4. Results and discussion

This section discusses the obtained results in this manuscript to explain their novelty and accuracy. This investigation depends on three items as shown:

- **Comparing the MKhat and MJE method's solutions with each other:**
  Accuracy investigation of our obtained solutions shows a variety of distinct solutions in different formulas such as rational, exponential, and trigonometric. This wide range of solutions covers a big area of the (2+1)-D CNLS equation's characterization.
- **Comparing our solutions with previous known results:**
  Comparing our solutions with those that have been evaluated in

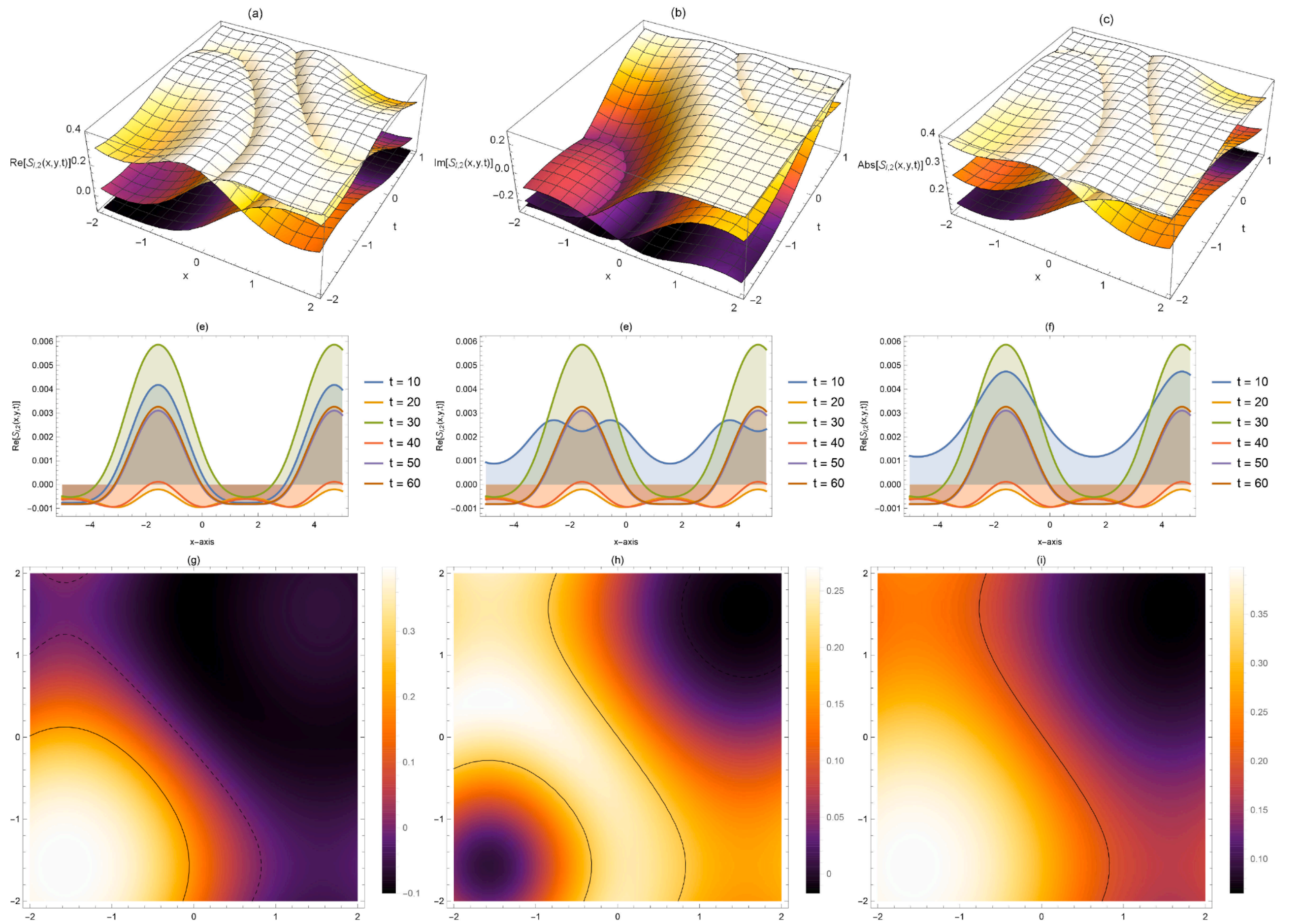

Fig. 4. Distinct plots in three, two–dimensional and contour plots of Eq. (18) for (a, d, g) real, (b, e, h) imaginary, and (c, f, i) absolute value of the solution with the following values $(a_1 = 0.4, g_1 = 0.9, g_2 = 0.8, g_3 = 0.8, g_4 = 0.7, g_5 = 0.6, g_6 = 0.5, \mathscr{L}_1 = 0.11, \mathscr{L}_2 = 0.1)$.

Table 1
Approximate simulation's results through the Mkhat and AD methods.

Value of $\mathfrak{z}$	Analytical	Approximate	Absolute Error
0	0	0	0
0.1	−0.069941725	−0.069941725	2.72166E−12
0.2	−0.139535192	−0.139535193	6.92808E−10
0.3	−0.208439047	−0.208439065	1.76391E−08
0.4	−0.276325448	−0.276325623	1.74879E−07
0.5	−0.342886127	−0.342887161	1.03373E−06
0.6	−0.407837657	−0.407842062	4.40453E−06
0.7	−0.470925762	−0.470940731	1.49687E−05
0.8	−0.531928547	−0.53197165	4.3103E−05
0.9	−0.590658607	−0.590767951	0.000109344
1	−0.64696402	−0.647214975	0.000250955
1.1	−0.700728296	−0.701259358	0.000531063
1.2	−0.751869394	−0.752920185	0.001050791
1.3	−0.800337953	−0.802302708	0.001964755
1.4	−0.846114888	−0.849615055	0.003500167
1.5	−0.889208533	−0.895188162	0.005979629
1.6	−0.929651478	−0.939498943	0.009847465
1.7	−0.967497258	−0.983196407	0.015699149
1.8	−1.002817018	−1.027130035	0.024313016
1.9	−1.035696272	−1.072379286	0.036683015
2	−1.066231818	−1.120282569	0.054050751

Table 2
Approximate simulation's results through the MJE and AD methods.

Value of $\mathfrak{z}$	Analytical	Approximate	Absolute Error
0	7	7	0
0.01	6.999650015	6.999650137	1.22501E−07
0.02	6.998600233	6.998602193	1.96004E−06
0.03	6.996851181	6.996861104	9.92297E−06
0.04	6.994403731	6.994435094	3.13626E−05
0.05	6.991259105	6.991335678	7.65725E−05
0.06	6.987418872	6.987577662	0.00015879
0.07	6.982884945	6.983179143	0.000294198
0.08	6.977659578	6.978161506	0.000501928
0.09	6.971745367	6.97254943	0.000804062
0.1	6.965145243	6.966370882	0.001225639
0.11	6.957862469	6.959657123	0.001794654
0.12	6.949900639	6.952442705	0.002542066
0.13	6.941263671	6.944765472	0.0035018
0.14	6.931955803	6.936666559	0.004710756
0.15	6.921981587	6.928190397	0.00620881
0.16	6.911345886	6.919384709	0.008038823
0.17	6.900053865	6.91030051	0.010246645
0.18	6.88811099	6.900992113	0.012881123
0.19	6.875523016	6.891517124	0.015994108
0.2	6.862295984	6.881936444	0.019640461

[35] which has applied the five direct test functions, shows the difference between our and their solutions. Also, it shows a difference in our treatment of the same model where we have investigated the coefficient in the (2+1)-D CNLS equation as arbitrary constants but in [35], they have used these coefficients as time-dependent.

- **Physical interpretation of the shown sketches:**

  Investigation the physical interpretation of the shown figures of the computational solutions is giving by.

  1. Fig. 1 shows periodic wave solutions of the real, imaginary, and absolute parts of the expression in Eq. (8) under the following

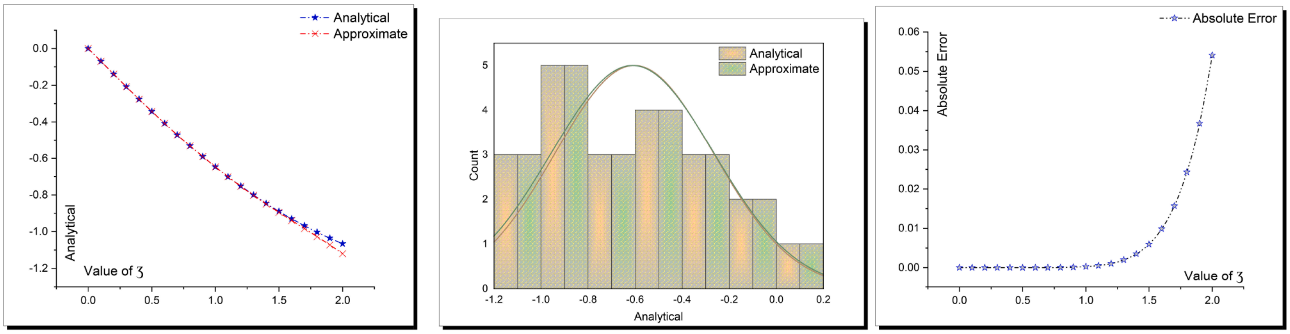

Fig. 5. Matching between analytical and approximate solutions (Khat method Vs AD method).

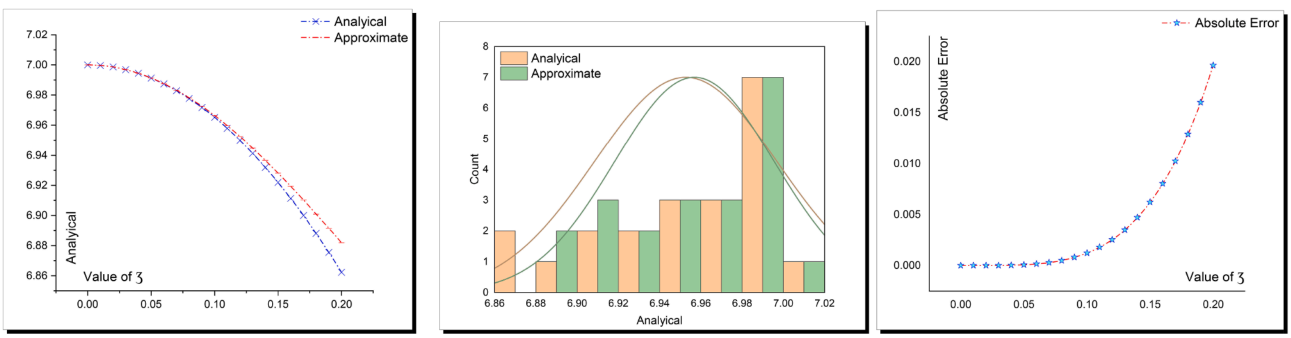

Fig. 6. Matching between analytical and approximate solutions (MJE method Vs AD method).

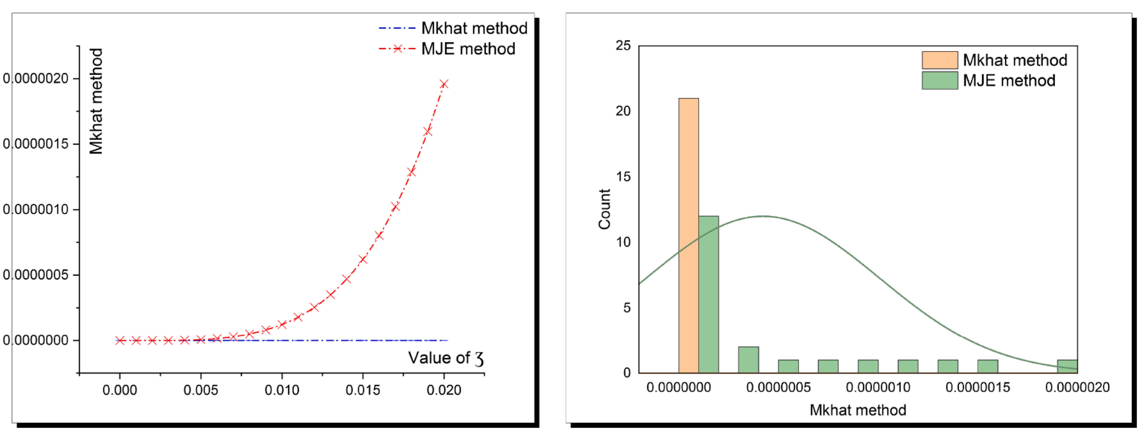

Fig. 7. (MJE method Vs AD method)'s superiority.

values of the above–shown parameters $\big[a_0 = 11, d_2 = 5, d_1 = 3,$

$$d_3 = 2, g_1 = 5, g_2 = 6, g_3 = 4, g_4 = 3, g_5 = 9, g_6 = 10, \mathscr{L}_1 = 7, \mathscr{L}_2 = 8\big]$$

.

2. Fig. 2 shows kink wave solutions of the real, imaginary, and absolute parts of the expression in Eq. (10) under the following values of the above–shown parameters $\big[a_1 = 0.4, g_1 = 0.9, g_2 = 0.8,$

$$g_3 = 0.8, g_4 = 0.7, g_5 = 0.6, g_6 = 0.5, \mathscr{L}_1 = 0.11, \mathscr{L}_2 = 0.1\big]$$

.

3. Fig. 3 shows cuspons wave solutions of the real, imaginary, and absolute parts of the expression in Eq. (16) under the following values of the above–shown parameters $\big[a_1 = 0.4, g_1 = 0.9,$

$$g_2 = 0.8, g_3 = 0.8, g_4 = 0.7, g_5 = 0.6, g_6 = 0.5, \mathscr{L}_1 = 0.11, \mathscr{L}_2 = 0.1\big]$$

.

4. Fig. 4 shows kink wave solutions of the real, imaginary, and absolute parts of the expression in Eq. (18) under the following values of the above–shown parameters $\big[a_1 = 0.4, g_1 = 0.9,$

$$g_2 = 0.8, g_3 = 0.8, g_4 = 0.7, g_5 = 0.6, g_6 = 0.5, \mathscr{L}_1 = 0.11, \mathscr{L}_2 = 0.1\big]$$

.

- **Accuracy of the two employed schemes:**

  This paper is not restricted to obtaining the analytical solutions of the (2+1)-D CNLS equation but it also investigates the accuracy of these obtained solutions. The computational solutions have been used to evaluate the initial and boundary conditions that allows applying the AD method. Table 1, 2 and Figs. 5, 6 explain the matching between analytical and approximate solutions. Additionally, Fig. 7 shows the accuracy of both used analytical schemes and proof the superiority of the MKhat method over the MJE method where the MKhat method's absolute error is smaller than MJE method's absolute error.

5. Conclusions

In this paper we have investigated the analytical and approximate solutions of the (2+1)-D CNLS equation by employing the Mkhat, MJE, AD methods. Abundant solitary wave solutions have been constructed that define the edge states of the fractional quantum hall effect. Additionally, the computational solutions have been used to evaluate the initial and boundary conditions that allow the use of the AD approximate method for evaluating the numerical solutions and absolute error between exact and numerical solution. This study shows the accuracy of the analytical solutions. The analytical solutions have been illustrated in 2D, 3D, and density plots while the matching between exact and numerical solutions has been pointed up in 2D plots.

CRediT authorship contribution statement

B. Alshahrani: Conceptualization, Formal analysis, Methodology, Software, Writing - original draft, Writing - review & editing. **H.A. Yakout:** Conceptualization, Formal analysis, Validation, Writing - original draft, Writing - review & editing. **Mostafa M.A. Khater:** Conceptualization, Formal analysis, Investigation, Methodology, Software, Supervision, Validation, Writing - original draft, Writing - review & editing. **Abdel-Haleem Abdel-Aty:** Conceptualization, Formal analysis, Investigation, Methodology, Resources, Software, Supervision, Validation, Writing - original draft, Writing - review & editing. **Emad E. Mahmoud:** Formal analysis, Software, Validation, Writing - original draft, Writing - review & editing. **Dumitru Baleanu:** Conceptualization, Investigation, Resources, Supervision, Validation, Writing - original draft, Writing - review & editing. **Hichem Eleuch:** Conceptualization, Investigation, Resources, Validation, Writing - original draft, Writing - review & editing.

Declaration of Competing Interest

The authors declare that they have no known competing financial interests or personal relationships that could have appeared to influence the work reported in this paper.

Acknowledgments

The authors extend their appreciation to the Deanship of Scientific Research at King Khalid University, Saudi Arabia for funding this work through Research Groups Program under Grant No. (R.G.P. 1/169/41). Emad E. Mahmoud acknowledges Taif University Researchers Supporting Project number (TURSP-2020/20), Taif University, Taif, Saudi Arabia.

References

[1] Al Khawaja U, Eleuch H, Bahlouli H. Analytical analysis of soliton propagation in microcavity wires. Results Phys 2019;12:471–4.
[2] Boutabba N, Eleuch H. Soliton-pair propagation under thermal bath effect. Math Model Nat Phenom 2012;7(2):32–7.
[3] Abdel-Aty A, Zakaria N, Cheong LY, Metwally N. Quantum network via partial entangled state. J Commun 2014;9:379–84.
[4] Khater MM. On the dynamics of strong langmuir turbulence through the five recent numerical schemes in the plasma physics. Numer Meth Partial Differ Eqs 2020.
[5] Wu L, Mousa A, Lu D, Khater M. Computational schemes between the exact, analytical and numerical solution in present of time-fractional ecological model. Phys Scr 2020.
[6] Singh H. A new stable algorithm for fractional Navier-Stokes equation in polar coordinate. Int J Appl Comput Math 2017;3(4):3705–22.
[7] Abdel-Aty A, Zakaria N, Cheong LY, Metwally N. Effect of the spin-orbit interaction on partial entangled quantum network. Lecture Notes Electr Eng 2014;285:529.
[8] Park C, Khater MM, Abdel-Aty A-H, Attia RAM, Rezazadeh H, Zidan A, Mohamed A-BM. Dynamical analysis of the nonlinear complex fractional emerging telecommunication model with higher-order dispersive cubic-quintic. Alex Eng Js 2020;28(8):2040035.
[9] Khater MM, Nisar KS, Mohamed MS. Numerical investigation for the fractional nonlinear space-time telegraph equation via the trigonometric Quintic B-spline scheme. Math Methods Appl Sci 2020.
[10] Boutabba N, Eleuch H, Bouchriha H. Thermal bath effect on soliton propagation in three-level atomic system. Synth Met 2009;159(13):1239–43.
[11] Khater MM, Almohsen B, Baleanu D, Inc M. Numerical simulations for the predator–prey model as a prototype of an excitable system. Numer Methods Partial Differ Eqs 2020.
[12] Khater MM, Hamed Y, Lu D. On rigorous computational and numerical solutions for the voltages of the electrified transmission range with the day yet distance. Numer Methods Partial Differ Eqs 2020.
[13] Singh H. Analysis for fractional dynamics of Ebola virus model. Chaos Solitons Fract 2020;138:109992.
[14] Abubakar M, Jung LT, Zakaria N, Younes A, Abdel-Aty A-H. Quantum circuit optimization using genetic programming with dynamic gate libraries. Quant Inf Process 2017;16:160–84.
[15] Khater M, Attia R, Abdel-Aty A. Computational analysis of a nonlinear fractional emerging telecommunication model with higher-order dispersive cubic-quintic. Inf Sci Lett 2020;9:83–93.
[16] Khater M, Baleanu D, Mohamed MS. Multiple lump novel and accurate analytical and numerical solutions of the three-dimensional potential Yu–Toda–Sasa–Fukuyama equation. Symmetry 2020;12(12):2081.
[17] Khater MM, Mohamed MS, Park C, Attia RA. Effective computational schemes for a mathematical model of relativistic electrons arising in the laser thermonuclear fusion. Results Phys 2020;19:103701.
[18] Singh H. Jacobi collocation method for the fractional advection-dispersion equation arising in porous media. Numer Methods Partial Differ Eqs 2020.
[19] Ali HM. An efficient approximate-analytical method to solve time-fractional kdv and kdvb equations. Inf Sci Lett 2020;9:189–98.
[20] Khater MM, Lu D, Hamed Y. Computational simulation for the (1+ 1)-dimensional Ito equation arising quantum mechanics and nonlinear optics. Results Phys 2020;19:103572.
[21] Singh H, Kumar D, Pandey RK. An efficient computational method for the time-space fractional Klein-Gordon equation. Front Phys 2020;8:281.
[22] Abdel-Aty A-H, Khater MM, Baleanu D, Abo-Dahab S, Bouslimi J, Omri M. Oblique explicit wave solutions of the fractional biological population (BP) and equal width (EW) models. Adv Differ Eqs 2020;2020(1):1–17.
[23] Al-Saif A, Abdul-Wahab M. Application of new simulation scheme for the nonlinear biological population model. Numer Comput Meth Sci Eng 2019;1:89.
[24] Abdel-Aty A-H, Khater MM, Baleanu D, Khalil E, Bouslimi J, Omri M. Abundant distinct types of solutions for the nervous biological fractional Fitzhugh-Nagumo equation via three different sorts of schemes. Adv Differ Eqs 2020;2020(1):1–17.
[25] Salah R, Anwer MM, Abdel-Aty M. Pancharatnam phase of non-hermitian hamiltonian. Inf Sci Lett 2021;10:25–32.
[26] Khater MM, Baleanu D. On abundant new solutions of two fractional complex models. Adv Differ Eqs 2020;2020(1):1–14.
[27] Yue C, Khater MM, Attia RA, Lu D. The plethora of explicit solutions of the fractional KS equation through liquid–gas bubbles mix under the thermodynamic conditions via atangana–baleanu derivative operator. Adv Differ Eqs 2020;2020(1):1–12.
[28] Hermann J, Schätzle Z, Noé F. Deep-neural-network solution of the electronic Schrödinger equation. Nat Chem 2020;12(10):891–7.
[29] Pfau D, Spencer JS, Matthews AG, Foulkes WMC. Ab initio solution of the many-electron Schrödinger equation with deep neural networks. Phys Rev Res 2020;2(3):033429.
[30] Qiu Y, Malomed BA, Mihalache D, Zhu X, Peng X, He Y. Stabilization of single-and multi-peak solitons in the fractional nonlinear Schrödinger equation with a trapping potential. Chaos Solitons Fract 2020;140:110222.
[31] Wang B-H, Lu P-H, Dai C-Q, Chen Y-X. Vector optical soliton and periodic solutions of a coupled fractional nonlinear Schrödinger equation. Results Phys 2020;103036.
[32] Khater MM, Attia RA, Abdel-Aty A-H, Abdou M, Eleuch H, Lu D. Analytical and semi-analytical ample solutions of the higher-order nonlinear Schrödinger equation with the non-kerr nonlinear term. Results Phys 2020;16:103000.
[33] Li B-Q, Ma Y-L. Extended generalized darboux transformation to hybrid rogue wave and breather solutions for a nonlinear Schrödinger equation. Appl Math Comput 2020;386:125469.
[34] Arshed S, Arif A. Soliton solutions of higher-order nonlinear Schrödinger equation (NLSE) and nonlinear Kudryashov's equation. Optik 2020;209:164588.
[35] Sulaiman TA, Yusuf A, Abdel-Khalek S, Bayram M, Ahmad H. Nonautonomous complex wave solutions to the (2+1)-dimensional variable-coefficients nonlinear chiral Schrödinger equation. Results Phys 2020;19:103604.